Week 10
Lecture Notes:
Topological Condensed Matter Physics

Sebastian Huber and Titus Neupert

Department of Physics, ETH Zürich
Department of Physics, University of Zürich

Chapter 10

Topological semimetals

Learning goals

- We know Weyl semimetals, their Fermi arc surface states and chiral anomaly.
- We have an overview of other types of symmetry-enforced degeneracies in band structures, including point-like degeneracies of several bands and nodal lines.

- X. Wan, et al., Phys. Rev. B **83**, 205101 (2011)
- B. Bradlyn *et al.*, Science **353**, aaf5037 (2017)
- G. Chang *et al.*, Nature Mater. **17**, 978–985 (2018)

So far, this entire lecture was focussed on the topology in gapped ground states of matter. In this chapter we discuss gapless topological states, so-called topological semimetals. Remembering that topology was initially defined as (symmetry-protected) equivalence classes states under adiabatic deformations, this provokes the question what meaning we should attach to the adiabatic theorem in a gapless phase and – as a consequence – how topology should be defined at all in such a case. At least for the purpose of this lecture, we rescue the notion of topology by relying on translation symmetry. Hence we can label our Hamiltonian by momentum $\boldsymbol{k}$. (We used translation symmetry before, but mainly to obtain convenient formulas for topological invariants. The notion of the topological phases themselves was – with the exception of TQC – never dependent on translation symmetry.)
The story of topological semimetals is most interesting in three dimensions, which is why we focus on this case exclusively here. While the Hamiltonian, depending on three components of momentum, is then gapped almost everywhere in the BZ, the few points or lines where this is not the case are our main interest. At these nodal points or lines bands are degenerate and we will see that these degeneracies are *topologically stable*. They cannot be removed (yet potentially moved in the BZ), if the Hamiltonian is smoothly deformed while maintaining translation symmetry (and potentially some other protecting symmetries). Such a notion of robustness to deformations allows to define a *gapless phase* and a sense of topology.

10.1 Weyl semimetals

The Weyl semimetal is the most elementary topological semimetal, as we will see. A Hamiltonian for it can be motivated from several angles. Here we choose a perspective where we start from a three-dimensional topological insulator Hamiltonian in momentum space

$$\mathcal{H}_{\mathrm{TI}}(\boldsymbol{k}) = \sum_{i=x,y,z} \sin\, k_i\, \sigma_i \tau_x + \left(M - \sum_{i=x,y,z} \cos\, k_i \right) \sigma_0 \tau_z, \tag{10.1.1}$$

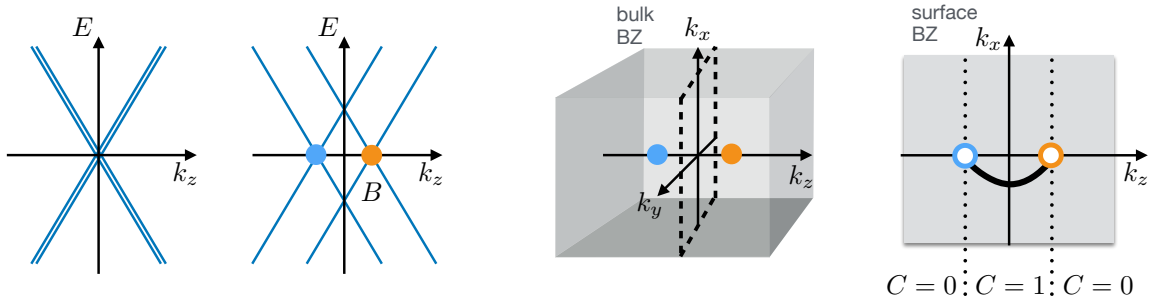

Figure 10.1: Momentum space picture of a Weyl semimetals. Left: The band structure of the critical point between a three-dimensional topological insulator and a trivial insulator is a gapless Dirac fermion. Upon the application of a Zeeman field, the Dirac fermion splits into two Weyl fermions (blue and orange) of opposite chiral charge. Right: The occupied bands on planes in momentum space that do not pass through the Weyl fermions carry a well-defined Chern number. This Chern number is $|C| = 1$ between two two Weyl points and 0 for planes outside. Correspondingly, there is a Fermi arc surface state in the surface BZ connecting the projections of the bulk Weyl points.

with time-reversal symmetry defined as

$$(\sigma_y\tau_0)\mathcal{H}^*_{\mathrm{TI}}(\boldsymbol{k})(\sigma_y\tau_0)^{-1} = \mathcal{H}_{\mathrm{TI}}(-\boldsymbol{k}) \tag{10.1.2}$$

and inversion symmetry defined as

$$(\sigma_0\tau_z)\mathcal{H}_{\mathrm{TI}}(\boldsymbol{k})(\sigma_0\tau_z)^{-1} = \mathcal{H}_{\mathrm{TI}}(-\boldsymbol{k}). \tag{10.1.3}$$

Here, σ_i are the Pauli matrices acting on the spin degree of freedom and τ_i are Pauli matrices that can be though of as acting on an s/p orbital degree of freedom – consistent with the opposite inversion eigenvalue of the orbitals indicated by τ_z.
Hamiltonian (10.1.1) is constructed such that all terms anticommute, which makes it easy to obtain the doubly degenerate bands (the degeneracy is due to inversion and time-reversal, giving a local in $\boldsymbol{k}$ Kramers symmetry)

$$E_\pm(\boldsymbol{k}) = \pm\sqrt{\sum_{i=x,y,z}\sin^2 k_i + \left(M - \sum_{i=x,y,z}\cos k_i\right)^2}. \tag{10.1.4}$$

This indicates several gap-closing phase transitions, in particular for $1 < |M| < 3$ we have a topological insulator. At the phase transition, $M = 3$, we can expand the Hamiltonian to linear order in $\boldsymbol{k}$ and obtain a massless Dirac equation (we rotate the orbital basis $\tau_x \leftrightarrow \tau_z$ for convenience)

$$\mathcal{H}_{\mathrm{TI,eff}}(\boldsymbol{k}) = \begin{pmatrix} \boldsymbol{k}\cdot\boldsymbol{\sigma} & 0 \\ 0 & -\boldsymbol{k}\cdot\boldsymbol{\sigma} \end{pmatrix}. \tag{10.1.5}$$

This Block structure of the Dirac equation was noticed by Hermann Weyl (in Zurich), and the Fermion (two-spinor) described by each of the 2×2 blocks is known as Weyl fermion. We thus see that two Weyl fermions make up one massless Dirac fermion. The innocent minus sign between the two blocks is actually quite important, as we will see in a bit. Studying the effective dispersion of one Weyl fermion is now hindered by the fact that the two coincide both in energy and momentum. To "separate" them, we apply a Zeeman magnetic field, which could

be sourced by some spontaneous ferromagnetic order in the crystal. Choosing this, without loss of generality, to be oriented along the z direction, we have

$$\mathcal{H}_{2-\text{Weyl}}(\boldsymbol{k}) = \begin{pmatrix} \boldsymbol{k}\cdot\boldsymbol{\sigma} + B\sigma_z & 0 \\ 0 & -\boldsymbol{k}\cdot\boldsymbol{\sigma} + B\sigma_z \end{pmatrix}. \tag{10.1.6}$$

This Hamiltonian has now momentum-separated Weyl fermions: one at $k_z = B$ and one at $k_z = -B$. Near each of these two momenta, two bands touch with an effective $\boldsymbol{k}\cdot\boldsymbol{\sigma}$ dispersion around the touching point, while the other two bands are at energies $\pm 2B$, and thus not considered part of the low-energy theory. The $\boldsymbol{k}\cdot\boldsymbol{\sigma}$ linear touching of two bands in three-dimensional momentum space is a *Weyl point*.

A Weyl point has topological robustness. Any translation-symmetric *small* perturbation that we add to a Hamiltonian $\boldsymbol{k}\cdot\boldsymbol{\sigma}$ can only move, but never remove the Weyl point! We can see this by expanding an arbitrary small perturbation in the basis of the Pauli matrices as $\delta_0\sigma_0 + \boldsymbol{\delta}\boldsymbol{\sigma}$. Adding it to the Hamiltonian gives

$$\delta_0\sigma_0 + (\boldsymbol{k} + \boldsymbol{\delta})\cdot\boldsymbol{\sigma}, \tag{10.1.7}$$

which now has Weyl point at $\boldsymbol{k} = -\boldsymbol{\delta}$ at energy δ_0. Weyl points can, however, annihilate pairwise.

It is a nice exercise to analytically calculate the Berry curvature near a Weyl node with Hamiltonian $\pm\boldsymbol{k}\cdot\boldsymbol{\sigma}$. For the occupied band, it is given by

$$\boldsymbol{\mathcal{F}}(\boldsymbol{k}) = \mp\frac{\boldsymbol{k}}{4\pi|\boldsymbol{k}|^3}. \tag{10.1.8}$$

This results suggests the interpretation of the Weyl node as a *monopole* of Berry curvature in momentum space. The monopole charge is quantized: If we integrate the Berry flux over any closed surface that encloses one of these Weyl nodes (which amounts to calculating the Chern number of the occupied bands on such a surface) we obtain ∓ 1. The overall sign in the Weyl Hamiltonian is thus the sign of the monopole (or chiral) charge of the Weyl fermion.

It is instructive to consider the Hamiltonian $\mathcal{H}_{2-\text{Weyl}}(k_x, k_y, k_z)$ as describing two-dimensional systems in x-y space, while k_z is a "tuning parameter" of these systems. Each of these two-dimensional Hamiltonians describes a sensible physical system (i.e., it is local), which are gapped except at $k_z = \pm B$. What is the topology of these systems and is there a topological phase transition at $k_z = \pm B$? First, we notice that for each of our two-dimensional systems, the Chern number is well defined – we denote is by $C(k_z)$. To answer our topology question, we go back to the monopole property of the Weyl points and consider the one at $k_z = B$, for concreteness: We can enclose it with two (oppositely oriented) planes at $k_z = B - \epsilon$ and $k_z = B + \epsilon$. Since the system is gapped on each of these planes, they have each an integer Chern number $C(B-\epsilon)$, $C(B+\epsilon)$ (for $0 < \epsilon < 2B$. The Weyl monopole implies $C(B+\epsilon) - C(B-\epsilon) = \text{sgn}B$, with the minus sign coming from the opposite orientation. From the lattice model, we can deduce that $C(|k_z| > |B|) = 0$. Hence, we obtain

$$C(k_z) = \begin{cases} 0 & |k_z| > |B| \\ \text{sng}(B) & |k_z| < |B| \end{cases}. \tag{10.1.9}$$

Between the Weyl points, the two-dimensional system is thus as Chern insulator. Crucial for this is the breaking of time-reversal symmetry through the magnetic field (which preserves inversion symmetry).

For the Berry curvature, inversion symmetry implies

$$\boldsymbol{\mathcal{F}}(\boldsymbol{k}) = \boldsymbol{\mathcal{F}}(-\boldsymbol{k}), \tag{10.1.10}$$

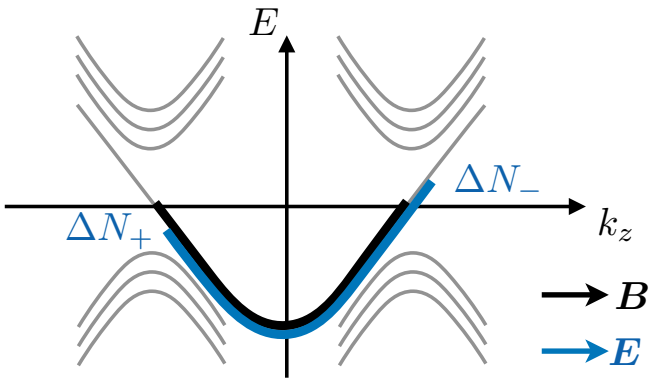

Figure 10.2: When a Weyl semimetal is expose to an orbital Zeeman field along the z direction, a k_z-dependent Landau level band structure forms (gray). In particular, one chiral and one antichiral Landau level pass through the Weyl points of monopole charge ± 1, respectively. When in addition an electrical field $\boldsymbol{E}$ is applied in parallel to the magnetic field, the resulting out-of-equilibrium, current-carrying state is depleting charge in one Weyl node and adding charge to the other Weyl node (blue). The chiral charge $N_+ - N_-$ is thus not conserved. This constitutes the chiral anomaly. The exchange of charge between the two Weyl nodes is allowed because the Landau levels at high energies connect the two Weyl nodes.

while time-reversal symmetry implies

$$\boldsymbol{\mathcal{F}}(\boldsymbol{k}) = -\boldsymbol{\mathcal{F}}(-\boldsymbol{k}). \tag{10.1.11}$$

One verifies that inversion (time-reversal) symmetry thus maps a Weyl cone of charge 1 at $\boldsymbol{k}$ to a cone at $-\boldsymbol{k}$ with charge -1 $(+1)$. Furthermore, the total charge of Weyl cones has to be zero in the entire BZ, due to its periodicity (a fact also conveyed by so-called Fermion doubling theorems). Thus, a time-reversal breaking Weyl semimetal (like our case), has at least two Weyl nodes, while an inversion-breaking Weyl semimetal has at least four Weyl cones. Furthermore, the combination of inversion and time-reversal symmetry implies $\boldsymbol{\mathcal{F}}(\boldsymbol{k}) \equiv 0$, in which case no Weyl nodes can exist.
Another important property of Weyl semimetals are *Fermi arcs*, their topological surface states. Since, $\mathcal{H}_{2-\mathrm{Weyl}}(k_x, k_y, k_z)$, $|k_z| < |B|$ has a nonzero Chern number, it has, as a two-dimensional system, chiral boundary states. In the two-dimensional surface BZ of the three-dimensional system, these states combine into a chiral surface band. This band is anomalous, i.e., it can only exist on the surface of a thee-dimensional object. One way to see this is by considering the Fermi surface they form: At the energy of the bulk Weyl points, the surface band's Fermi surface is a line connecting the surface BZ projections of the two Weyl points, the Fermi arc. In two-dimensional systems, Fermi surfaces are always closed contours. The way the Fermi arc evades this paradigm is by moving the other half of the closed contour Fermi surface to the opposite surface of the material.

10.1.1 Transport properties and the chiral anomaly

Weyl semimetals have peculiar transport properties. Most immediate is the anomalous Hall effect. Considering each k_z as independently contributing to Hall transport, we obtain an anomalous Hall conductivity

$$\sigma_{xy} = \frac{2B}{2\pi}\frac{e^2}{h}. \tag{10.1.12}$$

Note that the three-dimensional Hall conductivity has units of inverse length times e^2/h, i.e., it depends on the crystal details. Here, we see that it is proportional to the distance of the Weyl

nodes in k_z direction ($2B$).
More surprising is the effect of an *orbital* magnetic field on transport (note that what is in the Hamiltonian so far is a Zeeman magnetic field). The phenomenon that we will describe here, the *chiral anomaly*, is present both for small and large magnetic fields, but it is easier to understand in a large field limit, where Landau levels are well established.
To appreciate the deep meaning of the chiral anomaly, we make a small excursion to field theory. An *anomaly* is in general defined as a symmetry of the classical equations of motion that is not respected once quantum fluctuations are taken into account. Mathematically, in a path integral formulation, this is enabled by a symmetry of the action which is broken by the path integral measure. Concretely, the action for Dirac electrons in three-dimensional space, represented by a spinor-valued field ψ, is given by

$$S_{\text{Dirac}} = \int \mathrm{d}^4x\, \psi^\dagger \not{\nabla} \psi \tag{10.1.13}$$

with the covariant kinetic operator $\not{\nabla} = \gamma^\mu(\partial_\mu - A_\mu)$, where γ^μ are the Gamma matrices fulfilling the Clifford algebra and A_μ is the electromagnetic vector potential. The equations of motion

$$\not{\nabla}\psi = 0, \qquad \psi^\dagger \overleftarrow{\not{\nabla}} = 0, \tag{10.1.14}$$

feature, besides the $U(1)$ rotations with a unit matrix, leading to the conservation of charge, a so-called chiral symmetry

$$\psi \to e^{i\alpha\gamma_5}\psi, \tag{10.1.15}$$

where α is a real number. This leads to the chiral current

$$J_{\mu,5} := \psi^\dagger \gamma_\mu \gamma_5 \psi \tag{10.1.16}$$

to be classically conserved

$$\partial^\mu J_{\mu,5} = \psi^\dagger \overleftarrow{\not{\nabla}} \gamma_5 \psi - \psi^\dagger \gamma_5 \not{\nabla}\psi = 0. \tag{10.1.17}$$

However, when we compute the quantum average of this quantity with the full path integral

$$\begin{aligned} \langle \partial^\mu J_{\mu,5} \rangle =& \frac{\int \mathcal{D}[\psi]\mathcal{D}[\psi^\dagger] \left(\psi^\dagger \overleftarrow{\not{\nabla}} \gamma_5 \psi - \psi^\dagger \gamma_5 \not{\nabla}\psi \right) e^S_{\text{Dirac}}}{\int \mathcal{D}[\psi]\mathcal{D}[\psi^\dagger] e^S_{\text{Dirac}}} \\ =& \frac{1}{4\pi^2} \boldsymbol{E}\cdot\boldsymbol{B} \end{aligned} \tag{10.1.18}$$

we obtain a nonzero contribution if (non-orthogonal) electric and magnetic fields are simultaneously applied. The chiral current can be thought of as the difference between two currents of the chiral and antichiral part of the Fermion four-spinor. This is particularly apparent in the Dirac equation representation of Eq. (10.1.5), in which $\gamma_5 = \mathrm{diag}(1,1,-1,-1)$. It is thus the difference between the current of positive chirality Weyl fermions and the current of negative chirality Weyl fermions. Note that these currents are only well-defined in the continuum formulation of the Dirac equation. A fermion in a Weyl semimetal that lives at higher energies cannot be assigned to one or the other Weyl node.
This connection of the Weyl nodes at higher energies is what enables the chiral anomaly in a Weyl semimetal: Fermions can be pumped from one Weyl node to another through high-energy states when electric and magnetic fields are applied in parallel (see Fig. 10.1).
Finding unambiguous experimental proof of this fact has been proven difficult, with the most striking consequence found in semiclassical transport. One finds that the magnetoconductivity, i.e., the dependence of the conductivity on the applied magnetic field is highly anisotropic. It

has a quadratic magnetic field dependence that is maximal for transport along the magnetic field direction. Along the magnetic field direction the conductivity is modified from its zero field value σ_0 to

$$\sigma(B) = \sigma_0 + \frac{e^4 B^2 \tau_a}{4\pi^4 \nu(E_\mathrm{F})}, \tag{10.1.19}$$

where $\nu(E_\mathrm{F})$ is the density of states at the Fermi level and $1/\tau_a$ the rate of inter-Weyl node scattering. The most remarkable feature of this formula is the sign of the correction: this longitudinal magnetoconductivity is positive (and the longitudinal magnetoresistance thus negative). This is opposite to most other sources of magnetoresistance, where magnetic fields typically lead to increased localization and thus a larger resistivity.

10.1.2 Symmetry enforced Weyl nodes

We already discussed how time-reversal symmetry and inversion symmetry maps one Weyl node to another Weyl node of the same and opposite charge, respectively. This leaves the possibility open that a Weyl node is located at a time-reversal symmetric momentum. In fact, the generic time-reversal symmetric Hamiltonian of *any* spin orbit coupled band around *any* time-reversal symmetric momentum takes the form $A_{i,j}\, k_i \sigma_j$ with material-specific coefficients $A_{i,j}$ and is thus a Weyl node. The degeneracy at $\boldsymbol{k} = 0$ is then protected by Kramers theorem. These so-called Kramers-Weyl nodes are thus very abundant in band structures. However, they are only relevant in cases where spin orbit coupling is so strong that it is not immediately overtaken by the next order (k^2) term in the Hamiltonian which comes from the normal band dispersion. Kramers-Weyl semimetals have the advantage of (potentially) very long Fermi arcs, since their Weyl nodes are maximally far apart in the BZ. Furthermore, many lattice symmetries, such as mirror and inversion, prevent spin-orbit coupling from being nonzero in all directions in momentum space around the time-reversal invariant momentum. Kramers-Weyl nodes are thus preferably found in low-symmetry crystal structures, in particular in all chiral space groups (those without any mirror or (roto-)inversion).
We continue with some further constraints that crystal symmetries pose for Weyl nodes.

- **Mirror symmetry**: Just as a real magnetic field, the component of the Berry curvature parallel to the mirror plane is conserved, while the other components are flipped. Thus, no Weyl node can lie on a mirror plane in momentum space and mirror-related Weyl nodes on opposite sides of the mirror plane have opposite chiral charge. Another way to argue is that no unitary operation can reverse the sign of only one of the three Pauli matrices, as would be required for $\boldsymbol{k} \cdot \boldsymbol{\sigma}$ to be mirror symmetric.

- **Rotation symmetry**: Weyl nodes can exist on a rotation axis. However, depending on the rotation eigenvalues of the two bands that are coming together, Weyl nodes of higher charge may appear. In general, for a n-fold rotation symmetry, let the two bands have eigenvalues $e^{il_1/n}$ and $e^{il_2/n}$, with $l_1, l_2 = 0, 1, \cdots, n-1$. The chiral charge c of possible Weyl nodes between these two bands on the rotation axis is given by the difference in "angular momentum" $e^{ic/n} = e^{\pm i(l_1 - l_2)/n}$ (this relation also holds for spinful rotation symmetries where the eigenvalues are offset by a half-integer). An effective Hamiltonian for such a Weyl node of higher chiral charge is, for the case that the rotation axis is the z axis,

$$\mathcal{H}_{\mathrm{Weyl},c}(\boldsymbol{k}) = \begin{pmatrix} k_z & (k_x - ik_y)^c \\ (k_x + ik_y)^c & -k_z \end{pmatrix}. \tag{10.1.20}$$

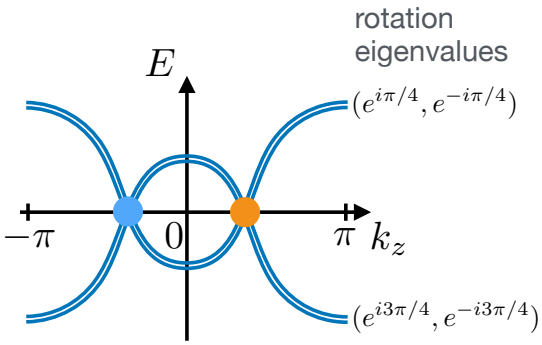

Figure 10.3: Band structure of the Dirac semimetal described by Eq. (10.2.2) for $k_x = k_y = 0$. The Dirac points are formed as doubly-degenerate pairs of bands with opposite rotation eigenvalues cross each other.

10.2 Dirac semimetals

Much like Weyl semimetals are materials where a band touching is described by the Weyl equation, there exist Dirac semimetals, in which a band touching (of four bands) is described by the massless Dirac equation (10.1.5). We previously obtained Eq. (10.1.5) as a critical point between a topological insulator and a trivial insulator phase. As such, the Dirac fermion is not topologically stable. To obtain a topologically stable massless Dirac fermion, we have to impose some symmetry on the system. We consider the case of four-fold rotation symmetry around the z axis as a concrete example and chose the representation

$$C_4 = \tau_z \exp\left[i\frac{\pi}{4}\sigma_z\right]. \tag{10.2.1}$$

One verifies that all terms in $\mathcal{H}_{\mathrm{TI}}(\boldsymbol{k})$ from Eq. (10.1.1) obey this C_4 symmetry, except for the $\sin k_z$ term. We thus consider the Hamiltonian without this term,

$$\mathcal{H}_{\mathrm{Dirac-SM}}(\boldsymbol{k}) = \sin k_x\, \sigma_x\tau_x + \sin k_y\, \sigma_y\tau_x + \left(M - \sum_{i=x,y,z} \cos k_i\right) \sigma_0\tau_z, \tag{10.2.2}$$

which obeys

$$C_4 \mathcal{H}_{\mathrm{Dirac-SM}}(R_4\boldsymbol{k}) C_4^{-1} = \mathcal{H}_{\mathrm{Dirac-SM}}(\boldsymbol{k}), \tag{10.2.3}$$

where R_4 is the four-fold rotation matrix in three-dimensional Euclidian space.
All bands of $\mathcal{H}_{\mathrm{Dirac-SM}}(\boldsymbol{k})$ are doubly degenerate everywhere, since we still have time-reversal and inversion symmetry. These doubly degenerate bands can touch at two points in the BZ. To see this, it is sufficient to consider the spectrum at the $(k_x, k_y) = (0, 0)$ line. It is given by

$$E_\pm(0, 0, k_z) = \pm\left(M - 2 - \cos k_z\right). \tag{10.2.4}$$

For $1 < M < 2$, there are two of these degeneracy points, which are Dirac points. Let us denote their k_z momenta by $\pm k_z^{\mathrm{D}}$. They are the crossing points of two bands with different C_4 eigenvalues (one band pair has $e^{\pm i\pi/4}$, another one has $e^{\pm i3\pi/4}$). Thus, as long as C_4 symmetry is maintained, the degeneracies cannot be removed or split by small (time-reversal-, inversion- and translation-preserving) perturbations. These Dirac points are thus topologically stable, in contrast to the Dirac point that marked the phase transition point.
Another way to characterize their topological property is by noting that for $1 < M < 2$, the Hamiltonian $\mathcal{H}_{\mathrm{Dirac-SM}}(\boldsymbol{k})$ at fixed k_z describes a two-dimensional topological insulator at $k_z = 0$

and a trivial insulator at $k_z = \pi$. The Dirac point thus marks the phase transition point between the two (when k_z is viewed as a tuning parameter). This argument has one potential flaw: in contrast to the Weyl semimetal, where Chern insulator topology was well-defined at every k_z slice, we require time-reversal symmetry to define the two-dimensional topological insulator, which a priori is only true for $k_z = 0, \pi$.

10.3 New fermions

We observed that Kramers-Weyl fermions can form at (and are pinned to) high-symmetry points in the BZ as two-fold band degeneracies. One may ask which higher band degeneracies are possibly enforced at high-symmetry points in the BZ if crystalline symmetries are considered in addition to time-reversal. The answer to this question is rather rich and has been determined for spin-orbit coupled band structures. One finds examples for $2-$, $3-$, $4-$, $6-$ and even $8-$fold protected degeneracies of bands, also known as *new Fermions*. One intuitive example is a degeneracy of three bands with the effective Hamiltonian

$$\mathcal{H}_{\text{spin}-1}(\boldsymbol{k}) = \boldsymbol{k} \cdot \boldsymbol{S}, \tag{10.3.1}$$

where S_i are the generators of the rotation group SO(3) in the spin-1 representation, which are 3×3 matrices. (This example appears in space groups 199 and 214.) The Chern numbers of each of the bands, obtained by integrating the Berry curvature over any surface enclosing the degeneracy point, are $C = \pm 2$ and $C = 0$. The degeneracy is thus not characterized by a single charge anymore, but a set of such charges.

10.4 Nodal line semimetals

In addition to degeneracy points, we can also consider degeneracies of bands along lines in momentum space. There is ample literature analyzing many aspects of this subject. Here, we just mention that a frequent mechanism for the protection of such nodal lines is the existence of a mirror symmetry. The line degeneracy can then be deformed within the mirror plane in momentum space, but cannot be removed by a small perturbation. Concretely, let us consider a two-band effective Hamiltonian, and consider a mirror operation $z \to -z$, i.e.,

$$M_z \mathcal{H}(k_x, k_y, -k_z) M_z^{-1} = \mathcal{H}(k_x, k_y, k_z). \tag{10.4.1}$$

Without loss of generality, we further assume $M = \sigma_z$ (in a spin-orbit coupled system, we would have $M = \mathrm{i}\sigma_z$ for it to commute with time-reversal symmetry). On the mirror planes $k_z = 0, \pi$, the symmetry then prevents σ_x and σ_y from entering the Hamiltonian. Degeneracies are thus zeros of the real function $d_z(k_x, k_y)$ in a Hamiltonian of the form

$$\mathcal{H}(k_x, k_y, 0, \pi) = d_0(k_x, k_y)\sigma_0 + d_z(k_x, k_y)\sigma_z. \tag{10.4.2}$$

Zeros of a scalar real function in two-dimensional parameter space are generically lines – the nodal line band degeneracies. Away from the mirror plane, there is no local (in $\boldsymbol{k}$) symmetry constraint on the Hamiltonian and the line-like degeneracy can thus gap out. It is confined to the mirror plane.

References

1. Wan, X., Turner, A. M., Vishwanath, A. & Savrasov, S. Y. "Topological semimetal and Fermi-arc surface states in the electronic structure of pyrochlore iridates". *Phys. Rev. B* **83,** 205101. http://link.aps.org/doi/10.1103/PhysRevB.83.205101 (2011).

2. Bradlyn, B. *et al.* "Topological quantum chemistry". *Nature* **537,** 298. https://dx.doi.org/10.1038/nature23268 (2017).

3. Chang, G. *et al.* "Topological quantum properties of chiral crystals". *Nature Mat.* **17,** 978. https://www.nature.com/articles/s41563-018-0169-3 (2018).